

# Quark Spectral Function and Deconfinement at Nonzero Temperature

Si-xue Qin<sup>1,\*</sup> and Dirk H. Rischke<sup>1,2,†</sup>

<sup>1</sup>*Institute for Theoretical Physics, Johann Wolfgang Goethe University,  
Max-von-Laue-Str. 1, D-60438 Frankfurt am Main, Germany*

<sup>2</sup>*Frankfurt Institute for Advanced Studies, Ruth-Moufang-Str. 1, D-60438 Frankfurt am Main, Germany*  
(Dated: February 25, 2022)

The maximum entropy method is used to compute the quark spectral function at nonzero temperature. We solve the gap equation of quantum chromodynamics (QCD) self-consistently, employing a rainbow kernel which phenomenologically models results from Dyson-Schwinger equations (DSE) and lattice QCD. We use the criterion of positivity restoration of the spectral function as a signal for deconfinement. Our calculation indicates that the critical temperature of deconfinement  $T_d$  is slightly smaller than the one of chiral symmetry restoration  $T_c$ :  $T_d \sim 94\%T_c$  in the chiral limit, and  $T_d \sim 96\%T_c$  with physical light quark masses. Since these deviations are within the systematic error of our approach, it is reasonable to conclude that chiral symmetry restoration and deconfinement coincide at zero chemical potential.

## I. INTRODUCTION

Heavy-ion experiments at the Relativistic Heavy-Ion Collider (RHIC) and the Large Hadron Collider (LHC) are focusing on charting the phase diagram of hot and dense nuclear matter. The quark-gluon plasma (QGP), a primordial state of matter in the early Universe, where chiral symmetry is restored and quarks and gluons are deconfined, has been re-created in the extremely hot environment of a heavy-ion collision. With the expansion of the fireball, nuclear matter cools down and dilutes. The low-temperature, low-density phase of nuclear matter is characterized by confinement and dynamical chiral symmetry breaking (DCSB). It is a central goal of modern theoretical physics to understand the properties of, and the transitions between, these phases. The chiral and deconfinement phase transitions as well as their interplay are especially interesting. In general, the chiral condensate (or, equivalently, the dynamical quark mass) is adopted as an order parameter for the chiral phase transition. The order of this transition may depend on the number of quark flavors, the values of the quark masses, and whether the  $U(1)_A$  anomaly of QCD is effectively restored. For nonzero quark masses, the existence of a critical end point (where the transition turns from being first order at low temperatures and high densities to being crossover at high temperatures and low densities) has been suggested but, even if it exists at all, its precise location is still highly debated.

Concerning the deconfinement phase transition, the situation is even more complicated because confinement has been a mystery since the inception of the Standard Model. The notion of confinement is easily understood from the linearly rising potential between infinitely heavy quarks [1, 2], which has also been studied by lattice QCD [3]. However, this is no longer true for light quarks

because of strong pair-creation and -annihilation effects [4]. In the pure-gauge limit realized for infinitely heavy quarks, the center  $Z(3)$  symmetry of the color gauge group  $SU(3)$  is preserved in the confining phase, while it is spontaneously broken in the deconfined phase. Here, the Polyakov loop (or the thermal Wilson line) [5, 6] is the corresponding order parameter. Equivalently, the dual quark condensate [7–9] was proposed as an order parameter, which makes it possible to study the interplay between confinement and DCSB. However, their validity as order parameters for phase transitions in light-quark systems remains unclear.

Besides these order parameters, confinement can be related to the analytic properties of QCD Schwinger functions [10–12]. The axiom of reflection positivity requires that the propagator must have a positive definite Källén-Lehmann spectral representation for asymptotic (or deconfined) quarks. In other words, if the quark propagator can be decomposed in terms of complete eigenstates of the Hamiltonian, each of which should have positive probability, quarks can propagate as asymptotic states; otherwise, quarks have to be somehow confined. It can be shown that pairs of complex conjugate poles of the full quark propagator lead to a nonpositive definite Källén-Lehmann spectral representation. Therefore, in Refs. [13, 14], the existence of such pairs of complex conjugate poles was considered as a criterion for confinement. However, this is only a sufficient condition. The reason is that the violation of reflection positivity can also be realised by propagators with real poles, namely if they have a negative residue which also leads to the Källén-Lehmann spectral representation being not positive definite [15]. On the other hand, the positivity of the quark spectral function is a necessary and sufficient condition for quark deconfinement, no matter whether the singularities of the quark propagator are located on or off the real axis. In short, by considering the quark spectral function directly, one is able to distinguish confined phases (where reflection positivity is violated) from deconfined ones (where reflection positivity holds).

In this work, we use the maximum entropy method

\* sixueqin@th.physik.uni-frankfurt.de

† drischke@th.physik.uni-frankfurt.de

(MEM) [16–19] to explicitly compute quark spectral functions from the self-consistent numerical solution of the QCD gap equation. We employ a rainbow kernel [20, 21] which phenomenologically models recent results from DSE [22, 23] and lattice QCD [24–26]. We define a deconfinement temperature as the temperature above which the positivity of the quark spectral function is restored. This work is a continuation of Ref. [27] where the quark spectral functions were studied in the region above  $T_c$ . This paper is organized as follows. In Sec. II, we present the QCD gap equation and discuss the *ansatz* employed for its solution. In Sec. III, we derive the relation between the quark spectral function and the solution of the gap equation. Here, we also define the order parameter which signals the positivity of the spectral function. In Sec. IV, we briefly outline the MEM and its extension for nonpositive definitive spectral functions. Section V reports our numerical results. Finally, we conclude with a summary and some remarks.

## II. QCD GAP EQUATION

At nonzero temperature, the QCD gap equation is

$$S(i\omega_n, \vec{p})^{-1} = i\vec{\gamma} \cdot \vec{p} + i\gamma_4\omega_n + m + \Sigma(i\omega_n, \vec{p}), \quad (1)$$

$$\Sigma(i\omega_n, \vec{p}) = \frac{4T}{3} \sum_{l=-\infty}^{+\infty} \int \frac{d^3\vec{q}}{(2\pi)^3} g^2 D_{\mu\nu}(\vec{k}, \Omega_{nl}) \times \gamma_\mu S(i\omega_l, \vec{q}) \Gamma_\nu(\vec{q}, \omega_l, \vec{p}, \omega_n), \quad (2)$$

where  $\omega_n = (2n+1)\pi T$  is the fermionic Matsubara frequency,  $\vec{k} = \vec{p} - \vec{q}$ ,  $\Omega_{nl} = \omega_n - \omega_l$ ,  $D_{\mu\nu}$  is the dressed gluon propagator, and  $\Gamma_\nu$  is the dressed quark-gluon vertex. The solution of the gap equation can be expressed as

$$S(i\omega_n, \vec{p})^{-1} = i\vec{\gamma} \cdot \vec{p} A(\omega_n^2, \vec{p}^2) + i\gamma_4\omega_n C(\omega_n^2, \vec{p}^2) + B(\omega_n^2, \vec{p}^2) \quad (3)$$

or, equivalently,

$$S(i\omega_n, \vec{p}) = -i\vec{\gamma} \cdot \vec{p} \sigma_A(\omega_n^2, \vec{p}^2) - i\gamma_4\omega_n \sigma_C(\omega_n^2, \vec{p}^2) + \sigma_B(\omega_n^2, \vec{p}^2), \quad (4)$$

where  $A, B, C$ , and  $\sigma_{A,B,C}$  are scalar functions. The dynamical quark mass is defined as  $M(\omega_n^2, \vec{p}^2) = B(\omega_n^2, \vec{p}^2)/A(\omega_n^2, \vec{p}^2)$ , which is independent of the renormalization point. In the chiral limit, the chiral condensate is defined as

$$-\langle \bar{q}q \rangle^0 = N_c T \sum_{n=-\infty}^{+\infty} \int \frac{d^3\vec{p}}{(2\pi)^3} \text{tr}_D S(i\omega_n, \vec{p}),$$

$$\sim M(\omega_0^2, \vec{p}^2 = 0). \quad (5)$$

However, because of an ultraviolet divergence the integral in the above equation is not well defined at nonzero current quark mass. Conveniently,  $M_0 := M(\omega_0^2, \vec{p}^2 = 0)$  can be used as the order parameter for the chiral phase transition, which is equivalent to the chiral condensate.

The gap equation is closed by specifying the vertex and the gluon propagator. Here, we use the rainbow truncation, i.e., the leading term in a symmetry-preserving scheme [28]:

$$g^2 D_{\mu\nu}(\vec{k}, \Omega_{nl}) \Gamma_\nu(\vec{q}, \omega_l, \vec{p}, \omega_n) = [P_{\mu\nu}^T D_T(\vec{k}^2, \Omega_{nl}^2) + P_{\mu\nu}^L D_L(\vec{k}^2, \Omega_{nl}^2)] \gamma_\nu, \quad (6)$$

where  $P_{\mu\nu}^{T,L}$  are transverse and longitudinal projection operators, respectively,

$$P_{\mu\nu}^T = \begin{cases} 0, & \mu \text{ and/or } \nu = 4, \\ \delta_{ij} - \frac{\vec{k}_i \vec{k}_j}{\vec{k}^2}, & \mu, \nu = 1, 2, 3, \end{cases} \quad (7)$$

$$P_{\mu\nu}^L = \delta_{\mu\nu} - \frac{k_\mu^\mu k_\nu^\nu}{k_\Omega^2} - P_{\mu\nu}^T, \quad (8)$$

with  $k_\Omega := (\Omega_{nl}, \vec{k})$ , and where

$$D_T = \mathcal{D}(\vec{k}^2 + \Omega_{nl}^2), \quad D_L = \mathcal{D}(\vec{k}^2 + \Omega_{nl}^2 + m_g^2). \quad (9)$$

Here, the function

$$\mathcal{D}(s) = \frac{8\pi^2 D}{\sigma^4} e^{-s/\sigma^2} + \frac{8\pi^2 \gamma_m}{\ln[\tau + (1 + s/\Lambda_{\text{QCD}}^2)^2]} \mathcal{F}(s), \quad (10)$$

with  $\mathcal{F}(s) = [1 - \exp(-s/4m_t^2)]/s$ ,  $\tau = e^2 - 1$ ,  $m_t = 0.5 \text{ GeV}$ ,  $\gamma_m = 12/25$ , and  $\Lambda_{\text{QCD}}^{N_f=4} = 0.234 \text{ GeV}$ . For pseudoscalar and vector mesons with masses  $\lesssim 1 \text{ GeV}$ , this interaction provides a uniformly good description of their vacuum properties when  $\sigma D = (0.8 \text{ GeV})^3$  and  $\sigma \in [0.4, 0.6] \text{ GeV}$  [20, 21], which means that there is only one free parameter in the model. The physical masses of the light quarks are  $m_{u=d}^\zeta = 3.4 \text{ MeV}$  at our renormalization point  $\zeta = 19 \text{ GeV}$ . Generalizing to  $T \neq 0$ , we have followed perturbation theory and included a Debye-like mass in the longitudinal part of the gluon propagator:  $m_g^2 = (16/5)T^2$  [for details, see Ref. [27]].

## III. SPECTRAL REPRESENTATION

The dressed quark propagator is related to the retarded real-time propagator by analytic continuation,

$$S^R(\omega, \vec{p}) = S(i\omega_n, \vec{p})|_{i\omega_n \rightarrow \omega + i\epsilon}. \quad (11)$$

From the spectral representation of  $S^R(\omega, \vec{p})$ , i.e.,

$$\rho(\omega, \vec{p}) = -2\Im S^R(\omega, \vec{p}), \quad (12)$$

one immediately obtains

$$S(i\omega_n, \vec{p}) = \int_{-\infty}^{+\infty} \frac{d\omega'}{2\pi} \frac{\rho(\omega', \vec{p})}{i\omega_n - \omega'}. \quad (13)$$

According to Eq. (4), the spectral function can be decomposed as

$$\rho(\omega, \vec{p}) = -i\vec{\gamma} \cdot \vec{p} \rho_v(\omega, \vec{p}^2) + \gamma_4 \omega \rho_e(\omega, \vec{p}^2) + \rho_s(\omega, \vec{p}^2). \quad (14)$$

As a consequence of the anti-commutation relation, the spectral function fulfills the following sum rule,

$$\int_{-\infty}^{+\infty} \frac{d\omega}{2\pi} \rho(\omega, \vec{p}) \gamma_4 = \mathbf{1}. \quad (15)$$

Then one can define the spectral function  $\rho_0(\omega, \vec{p}^2) := \omega \rho_e(\omega, \vec{p}^2)$ , which is nonnegative and can be treated as a probability distribution for deconfined quarks. Note that  $\rho_0(\omega, \vec{p}^2)$  can be easily related to the dressed quark propagator by

$$\begin{aligned} S_0(\omega_n^2, \vec{p}^2) &= i\omega_n \sigma_C(\omega_n^2, \vec{p}^2), \\ &= \int_{-\infty}^{+\infty} \frac{d\omega'}{2\pi} \frac{\rho_0(\omega', \vec{p}^2)}{\omega' - i\omega_n}, \end{aligned} \quad (16)$$

where  $\sigma_C$  is the scalar function in Eq. (4), or to the imaginary-time quark propagator

$$\begin{aligned} D_0(\tau, \vec{p}^2) &= T \sum_n e^{-i\omega_n \tau} S_0(\omega_n^2, \vec{p}^2), \\ &= \int_{-\infty}^{+\infty} \frac{d\omega}{2\pi} \frac{e^{(1/2 - \tau T)\omega/T}}{e^{\omega/2T} + e^{-\omega/2T}} \rho_0(\omega, \vec{p}^2). \end{aligned} \quad (17)$$

The above equations connect the quark spectral function which we consider to the numerical solution of the gap equation. As a signal for positivity violation (or restoration) of the spectral function, one can define an “order” parameter as

$$\hat{Z}_\rho = \int_{-\infty}^{+\infty} \frac{d\omega}{2\pi} |\rho(\omega)|, \quad (18)$$

$$Z_\rho = \int_{-\infty}^{+\infty} \frac{d\omega}{2\pi} \rho(\omega), \quad (19)$$

$$L_\rho = \frac{\hat{Z}_\rho - Z_\rho}{\hat{Z}_\rho}, \quad (20)$$

where  $\rho(\omega)$  simply denotes  $\rho_0(\omega, \vec{p}^2 = 0)$ . It is apparent that  $\hat{Z}_\rho = Z_\rho = 1$  and  $L_\rho = 0$  for a positive definite spectral function, otherwise  $\hat{Z}_\rho > Z_\rho = 1$  and  $L_\rho > 0$ . The critical temperature  $T_d$  of the deconfinement transition is defined as the lowest temperature where  $L_\rho = 0$ .

#### IV. MAXIMUM ENTROPY METHOD

It is an ill-posed problem to extract the spectral function from the (imaginary-time) quark propagator. Actually, there is an infinite set of spectral functions which can reproduce a given correlation function with tolerable errors. The MEM [16–19] considers the probability distribution of spectral functions to produce the most probable one. The theoretical basis is Bayes’ probability theorem. The conditional probability of having the spectral function  $\rho(\omega)$  given the correlation function  $D(\tau)$  reads

$$P[\rho|DM] = \frac{P[D|\rho M]P[\rho|M]}{P[D|M]}, \quad (21)$$

where  $M$  summarizes all definitions and prior knowledge of the spectral function,  $P[D|\rho M]$  and  $P[\rho|M]$  are called the likelihood function and the prior probability, respectively. Since  $P[D|M]$  is independent of  $\rho(\omega)$ , it can be treated as a normalization constant.

According to the central-limit theorem the data  $D(\tau)$  are expected to obey a Gaussian distribution:

$$P[D|\rho M] = \frac{1}{Z_L} e^{-L[\rho]}, \quad (22)$$

with

$$L[\rho] = \frac{1}{\beta} \int_0^\beta d\tau \frac{|D(\tau) - D[\rho](\tau)|^2}{2\xi(\tau)^2}, \quad (23)$$

where  $Z_L$  is a normalization constant,  $D[\rho]$  denotes the correlation function reproduced by Eqs. (16) or (17) given the spectral function  $\rho(\omega)$ , and  $\xi(\tau)$  is the variance of the error. Maximizing the likelihood function is equivalent to  $\chi^2$ -fitting.

The construction of the prior probability  $P[\rho|M]$  is the central idea of MEM, which expresses the prior in terms of the spectral entropy as

$$P[\rho|M(\alpha)] = \frac{1}{Z_S} e^{\alpha S[\rho, m]}, \quad (24)$$

where  $Z_S$  is a normalization constant and  $\alpha$  is an undetermined positive scale factor. The Shannon-Jaynes entropy  $S$  is defined as

$$S[\rho, m] = \int_{-\infty}^{+\infty} d\omega \left[ \rho(\omega) - m(\omega) - \rho(\omega) \ln \frac{\rho(\omega)}{m(\omega)} \right], \quad (25)$$

where  $m(\omega)$  is the “default model” of the spectral function. Its typical form is a uniform distribution without *a priori* structure assumption [27], i.e.,

$$m(\omega) = m_0 \theta(\Lambda^2 - \omega^2). \quad (26)$$

Note that a reliable output from the MEM should be insensitive to  $m_0$  and  $\Lambda$ . If the spectral function is not positive definite, one can decompose it in terms of two positive definite components, i.e.,

$$\rho(\omega) = \rho_+(\omega) - \rho_-(\omega), \quad (27)$$

Correspondingly, the total entropy is expressed as [29, 30]

$$S[\rho, m] = S[\rho_+, m_+] + S[\rho_-, m_-], \quad (28)$$

where  $m_\pm$  denotes the default models of  $\rho_\pm$ , respectively.

Finally, one obtains the total probability distribution

$$P[\rho|DM(\alpha)] \propto e^{\alpha S[\rho, m] - L[\rho]}. \quad (29)$$

The most probable spectral function  $\rho_\alpha(\omega)$  for fixed  $\alpha$  can be obtained by maximizing  $P[\rho|DM(\alpha)]$ , where usually the standard singular-value decomposition algorithm of Bryan [16] is adopted. To deal with the scale factor  $\alpha$ , we

follow Bryan's Method [16]. The MEM spectral function is defined as

$$\begin{aligned}\rho_{\text{MEM}} &= \int_0^\infty d\alpha \int \mathcal{D}\rho \rho(\omega) P[\rho|DM(\alpha)] P[\alpha|DM] \\ &\simeq \int_0^\infty d\alpha \rho_\alpha(\omega) P[\alpha|DM],\end{aligned}\quad (30)$$

where it is assumed that  $P[\rho|DM(\alpha)]$  is sharply peaked around  $\rho_\alpha(\omega)$ , so that the functional integral over  $\rho$  can be approximated. In this way, the MEM spectral function becomes an average of the  $\rho_\alpha(\omega)$ 's with respect to  $\alpha$ . The conditional probability  $P[\alpha|DM]$  can be evaluated using Bayes' theorem as

$$P[\alpha|DM] = \int \mathcal{D}\rho P[\rho|DM(\alpha)] P[\alpha|M] \quad (31)$$

$$\propto P[\alpha|M] \int \mathcal{D}\rho e^{\alpha S[\rho, m] - L[\rho]}. \quad (32)$$

Using the saddle-point approximation and the Laplace rule ( $P[\alpha|M] = \text{const}$ ), one obtains

$$P[\alpha|DM] \propto \exp\left(\frac{1}{2} \sum_k \ln \frac{\alpha}{\alpha + \lambda_k} + \alpha S[\rho_\alpha, m] - L[\rho_\alpha]\right),$$

where the  $\lambda_k$  are eigenvalues of the following real symmetric matrix in functional space

$$\Lambda_{ij} = \sqrt{\rho_i} \frac{\partial^2 L}{\partial \rho_i \partial \rho_j} \sqrt{\rho_j} \Big|_{\rho=\rho_\alpha}. \quad (33)$$

Normalizing  $P[\alpha|DM]$  and using Eq. (30) one finally obtains  $\rho_{\text{MEM}}$ .

## V. NUMERICAL RESULTS

At zero temperature,  $T = 0$ , the largest contribution to the constituent quark mass comes from DCSB which dominates low-energy hadron physics. With increasing temperature,  $T > 0$ , the dynamical quark mass decreases, which indicates a partial restoration of chiral symmetry. In the chiral limit, there exists a critical temperature  $T_c$  where the dynamical quark mass drops to zero and chiral symmetry is completely restored through a second-order phase transition [31]. Because of nonzero current quark masses, chiral symmetry is not exact. Instead of a second-order phase transition, a crossover happens at some pseudo-critical temperature  $T_c$  which is defined by the steepest-descent point for the dynamical quark mass. For these two cases, the behavior of the dynamical quark masses with temperature is illustrated in the upper panel of Fig. 1. The (pseudo-)critical temperatures have been indicated as vertical dashed lines.

Using our model parameters which are able to provide a uniformly good description of vacuum properties of pseudoscalar and vector mesons with masses  $\lesssim 1$  GeV, we calculate the dependence of the (pseudo-)critical temperatures on the interaction width  $\sigma$ , which is shown in

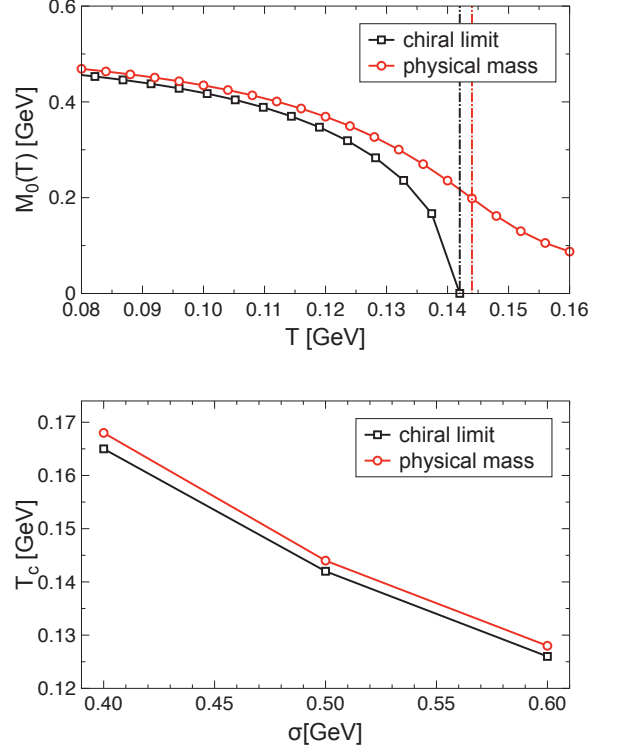


FIG. 1. (color online) Upper panel: behavior of the dynamical quark mass with temperature (for  $\sigma = 0.5$  GeV). The black line is the chiral limit, the red line is for the physical value of the current quark mass. The black dashed line denotes the critical temperature  $T_c$  of the second-order phase transition in the chiral limit, the red dashed line denotes the steepest-descent point for the dynamical quark mass, i.e., the pseudo-critical temperature for the physical current quark mass. Lower panel: Dependence of the (pseudo-)critical temperature  $T_c$  on the interaction width  $\sigma$  in our model.

the lower panel of Fig. 1:  $T_c$  monotonically decreases with increasing  $\sigma$ . This behavior is consistent with results obtained in Ref. [31]. Remarkably, the critical temperature range overlaps well with that obtained by lattice QCD, i.e.,  $T_c \in [0.146, 0.170]$  GeV [32].

Above the critical temperature  $T_c$ , the quark spectral function has been studied by both perturbative and non-perturbative approaches. At  $T > 3T_c$  where perturbation theory (hard-thermal-loop resummation) works, the properties of the QGP are dominated by two collective excitations: thermal and plasmino excitations [33]. At  $T \gtrsim T_c$ , experimental observables indicate that nuclear matter is a strongly-coupled QGP (sQGP) [34]. In this temperature region, perturbation theory fails while the nonperturbative DSE approach predicts a novel zero excitation mode in addition to the normal thermal and plasmino ones [27]. The typical behavior of the quark spectral function is illustrated in Fig. 2. Here, the spectral function is positive definite and each peak corresponds to an excitation mode.

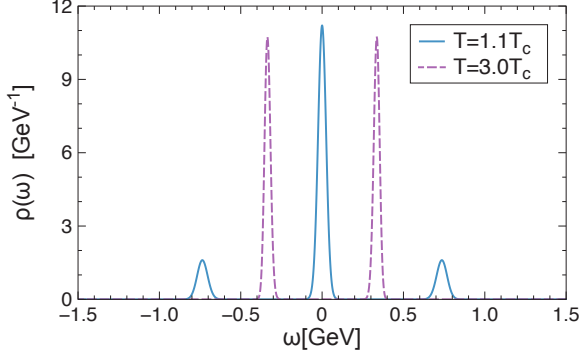


FIG. 2. (color online) Typical behavior of the spectral function at  $T > T_c$  (following Ref. [27]).

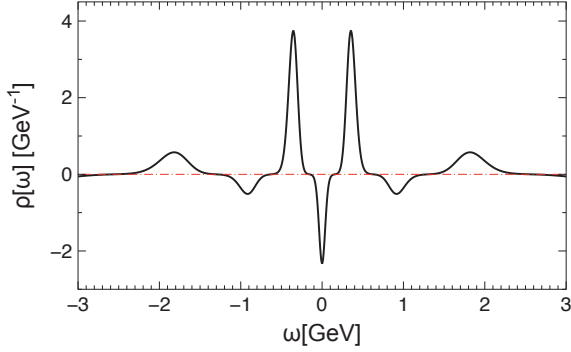


FIG. 3. (color online) The behavior of the quark spectral function at  $T = 0.8T_c$  ( $\sigma = 0.5$  GeV, chiral limit).

Below the critical temperature  $T_c$ , the system is non-perturbative because of DCSB and/or confinement. Nevertheless, the spectral function computed from the solution of the truncated gap equation can provide some non-trivial information about the system. We first calculate the quark spectral function at  $T = 0.8T_c$  with the interaction width  $\sigma = 0.5$  GeV and in the chiral limit, which is plotted in Fig. 3. It is found that the quark spectral function exhibits some negative peaks and thus obviously  $L_\rho > 0$ . Although the physical meaning of those negative peaks is unclear, it still makes sense to analyze how their behavior changes with temperature. We found that the structure of the nonpositive spectral function remains unchanged while the residues of the negative peaks, i.e.,  $L_\rho$ , decrease with increasing temperature. Notably, there exists a critical temperature  $T_d$  where  $L_\rho$  drops to zero, which signals the positivity restoration of the spectral function and deconfinement. The calculated behavior of  $L_\rho$  is shown in Fig. 4 in comparison with that of the dynamical mass  $M_0$ , which indicates that  $T_d \lesssim T_c$ . Next, we calculate the dependence of  $T_d$  on the interaction width  $\sigma$  both in the chiral limit and with a physical current quark mass, which is shown in Fig. 5:  $T_d$  monotonically

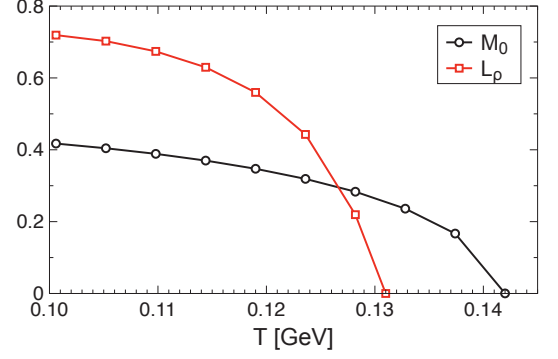


FIG. 4. (color online) The dynamical quark mass  $M_0$  and the deconfinement order parameter  $L_\rho$  as a function of temperature ( $\sigma = 0.5$  GeV, chiral limit).

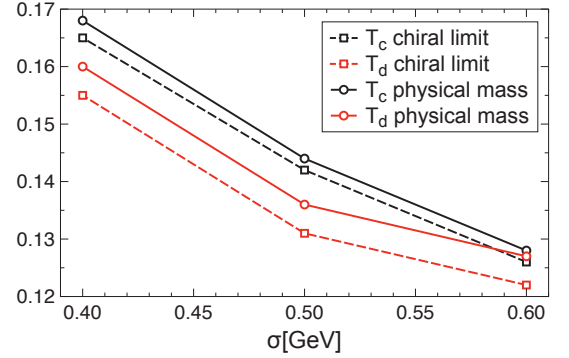


FIG. 5. (color online) The (pseudo-)critical temperature  $T_c$  (black) and the deconfinement temperature  $T_d$  (red) vs. the interaction width  $\sigma$  in the chiral limit (dashed lines) and for a physical current quark mass (full lines).

decreases with increasing  $\sigma$ , and  $T_d$  is slightly smaller than  $T_c$ . The difference between  $T_d$  and  $T_c$  for a physical current quark mass is smaller than that obtained in the chiral limit. Specifically, when  $\sigma \in [0.4, 0.6]$  GeV, we have  $T_d \sim 94\%T_c$  in the chiral limit and  $T_d \sim 96\%T_c$  with a physical light quark mass. The numerical results are presented in Table I. Our results are consistent with Ref. [18] which also found positivity violations of the Schwinger function below  $T_c$ .

TABLE I. Critical temperatures of chiral symmetry restoration  $T_c$  and deconfinement  $T_d$  for different parameters (dimensionful quantities reported in GeV,  $\Delta = T_c - T_d$ ).

$\sigma$	$T_c^0$	$T_d^0$	$\Delta^0/T_c^0$	$T_c^m$	$T_d^m$	$\Delta^m/T_c^m$
0.4	0.165	0.155	6.1%	0.168	0.160	4.8%
0.5	0.142	0.131	7.7%	0.144	0.136	5.6%
0.6	0.126	0.122	3.2%	0.128	0.127	0.8%
avg.	0.144	0.136	5.7%	0.147	0.141	3.7%



By defining a confinement scale  $r_\sigma = 1/\sigma$ , it is apparent that both  $T_c$  and  $T_d$  increase with increasing  $r_\sigma$ , or  $T_{c,d} \propto r_\sigma$ . Considering that the difference between  $T_c$  and  $T_d$  is just several MeVs, while the systematic uncertainty introduced by our approximations is certainly larger, it is reasonable to claim that chiral symmetry restoration and deconfinement coincide at nonzero temperature and zero chemical potential.

## VI. SUMMARY AND REMARKS

At nonzero temperature and zero chemical potential, we computed the quark spectral function via the MEM from a solution of the QCD gap equation. For the latter, we used a rainbow interaction kernel which phenomenologically models recent results from DSE and lattice QCD. As a criterion for the positivity violation and restoration of the quark spectral function, we proposed an order parameter  $L_\rho$  which is directly related to the integral of the spectral function's negative part and obviously vanishes for positive definite spectral functions. We indeed found that  $L_\rho > 0$  at low temperature while  $L_\rho \equiv 0$  at high temperature, i.e., there exists a critical temperature  $T_d$  where  $L_\rho$  drops to zero. Here, the

positivity of the quark spectral function is restored and quarks become asymptotic particles for  $T > T_d$ . Therefore, we conjecture that the deconfinement phase transition happens at  $T = T_d$ . Using our model setup, which can uniformly well describe vacuum properties of pseudoscalar and vector mesons with masses  $\lesssim 1$  GeV, the critical temperature of deconfinement comes out slightly smaller than that of chiral symmetry restoration, i.e.,  $T_d \lesssim T_c$ . Within the systematic uncertainties of our approach, however, it is reasonable to conclude that chiral symmetry restoration and deconfinement coincide.

It is generally expected that nuclear matter has a rich phase structure because of the interplay between DCSB and confinement at nonzero chemical potential. It would therefore be interesting to extend the present study to the case of nonzero chemical potential. The difference between  $T_c$  and  $T_d$  could then be more pronounced and give rise to the so-called quarkyonic phase [35, 36].

## ACKNOWLEDGEMENT

S.-x. Qin would like to thank C. S. Fischer and Y.-x. Liu for helpful discussions. The work of S.-x. Qin was supported by the Alexander von Humboldt Foundation through a Postdoctoral Research Fellowship.

- 
- [1] K. G. Wilson, Phys. Rev. D **10**, 2445 (1974).
  - [2] E. Eichten, K. Gottfried, T. Kinoshita, K. Lane, and T. Yan, Phys. Rev. D **17**, 3090 (1978).
  - [3] G. Bali, Phys. Rept. **343**, 1 (2001).
  - [4] G. Bali *et al.*, Phys. Rev. D **71**, 114513 (2005).
  - [5] B. Svetitsky and L. G. Yaffe, Nucl. Phys. B **210**, 423 (1982).
  - [6] R. D. Pisarski, Phys. Rev. D **62**, 111501 (2000).
  - [7] E. Bilgici, F. Bruckmann, C. Gattlinger, and C. Hagen, Phys. Rev. D **77**, 094007 (2008).
  - [8] C. S. Fischer, Phys. Rev. Lett. **103**, 052003 (2009).
  - [9] C. S. Fischer and J. A. Mueller, Phys. Rev. D **80**, 074029 (2009).
  - [10] C. D. Roberts, Int. J. Mod. Phys. A **7**, 5607 (1992).
  - [11] C. D. Roberts and A. G. Williams, Prog. Part. Nucl. Phys. **33**, 477 (1994).
  - [12] C. D. Roberts, Prog. Part. Nucl. Phys. **61**, 50 (2008).
  - [13] P. Maris, Phys. Rev. D **52**, 6087 (1995).
  - [14] M. Bhagwat, M. Pichowsky, and P. C. Tandy, Phys. Rev. D **67**, 054019 (2003).
  - [15] W. Yuan, S.-x. Qin, H. Chen, and Y.-x. Liu, Phys. Rev. D **81**, 114022 (2010).
  - [16] R. K. Bryan, Eur. Biophys. J. **18**, 165 (1990).
  - [17] D. Nickel, Ann. Phys. **322**, 1949 (2007).
  - [18] J. A. Mueller, C. S. Fischer, and D. Nickel, Eur. Phys. J. C **70**, 1037 (2010).
  - [19] M. Asakawa, T. Hatsuda, and Y. Nakahara, Prog. Part. Nucl. Phys. **46**, 459 (2001).
  - [20] S.-x. Qin, L. Chang, Y.-x. Liu, C. Roberts, and D. Wilson, Phys. Rev. C **84**, 042202 (2011).
  - [21] S.-x. Qin, L. Chang, Y.-x. Liu, C. D. Roberts, and D. J. Wilson, Phys. Rev. C **85**, 035202 (2012).
  - [22] A. Aguilar, D. Binosi, J. Papavassiliou, and J. Rodríguez-Quintero, Phys. Rev. D **80**, 085018 (2009).
  - [23] A. Aguilar, D. Binosi, and J. Papavassiliou, Phys. Rev. D **86**, 014032 (2012).
  - [24] P. O. Bowman, U. M. Heller, D. B. Leinweber, M. B. Parappilly, and A. G. Williams, Phys. Rev. D **70**, 034509 (2004).
  - [25] O. Oliveira and P. Bicudo, J. Phys. G: Nucl. Part. Phys. **38**, 045003 (2011).
  - [26] Ph. Boucaud *et al.*, Phys. Rev. D **82**, 054007 (2010).
  - [27] S.-x. Qin, L. Chang, Y.-x. Liu, and C. Roberts, Phys. Rev. D **84**, 014017 (2011).
  - [28] A. Bender, C. D. Roberts, and L. v. Smekal, Phys. Lett. B **380**, 7 (1996).
  - [29] M. Hobson and A. Lasenby, Mon. Not. R. Astron. Soc. **298**, 905 (1998).
  - [30] A. Balandin and A. Kaneko, Inverse Problems **15**, 445 (1999).
  - [31] S.-x. Qin, L. Chang, H. Chen, Y.-x. Liu, and C. D. Roberts, Phys. Rev. Lett. **106**, 172301 (2011).
  - [32] Y. Aoki *et al.*, JHEP **0906**, 088 (2009).
  - [33] M. Le Bellac, *Thermal Field Theory* (Cambridge University Press, 2000).
  - [34] H. Song and U. Heinz, J. Phys. G: Nucl. Part. Phys. **36**, 064033 (2009).
  - [35] L. McLerran and R. D. Pisarski, Nucl. Phys. A **796**, 83 (2007).
  - [36] L. McLerran, K. Redlich, and C. Sasaki, Nucl. Phys. A **824**, 86 (2009).